Advanced Multi-neural System for Cuff-less Blood Pressure Estimation through Nonlinear HC-features

Francesco Rundo[1][a], Alessandro Ortis[2][b], Sebastiano Battiato[2][c] and Sabrina Conoci[1][d]

[1]*STMicroelectronics, ADG Group – Central R&D, Str. Primosole, 50, 95121 Catania CT, Italy*
[2]*Dipartimento di Matematica e Informatica, Università Degli Studi di Catania, Viale A. Doria 6, 95125 - Catania, Italy*

Keywords: Blood Pressure Estimation, PPG, ECG.

Abstract: Blood Pressure (BP) is one of the most important physiological indicator that can provide useful information in the medical field. BP is usually measured by a sphygmomanometer device, which is composed by a cuff and a mechanical manometer. In this paper, a novel algorithmic approach to accurately estimate both systolic and diastolic blood pressure is presented. This algorithm exploits the PhotoPlethysmoGraphy (PPG) signal pattern acquired by non-invasive and cuff-less Physio-Probe (PP) silicon-based SiPM device. The PPG data are then processed with ad-hoc bio-inspired mathematical model which estimates both systolic and diastolic pressure values. We compared our results with those measured using a classical sphygmomanometer device and encouraging results of about 97% accuracy were achieved.

1 INTRODUCTION

The classical medical method to measure Blood Pressure (BP) is the use of the stethoscope. Recent cuff-based digital devices approaches are invasive, costly and do not allow continuous monitoring. Innovative methods try to estimate BP by analyzing the waves produced upon the heart dynamic along the arteries. In (Kurylyak, 2013) a non-invasive continuous BP estimation approach based on Artificial Neural Networks (ANNs) is proposed. The ANN is trained with 21 input parameters extracted from PPG signals. In (Yan, 2006) the authors described a new set of PPG hand-crafted features exhibiting encouraging results. The paper reported in (Gu, 2008) proposes an estimation of BP by means of new calibration parameters related to the dicrotic notch of the processed PPG waveform. The papers in (Teng, 2003) and in (Fortino, 2010) provide detailed surveys on the methodologies proposed in the literature for estimating BP from PPG signals. However, all these methodologies present the disadvantage that are based on PTT (Pulse Transit Time) calculation, which requires the sampling of both ECG (ElectroCardioGraphy) and PPG signals. Additionally, specific HW (PPG/ECG) sensors and SW (data extraction (PTT, PWV)) are needed. Finally, those methods may involve high computational costs against a reduced accuracy and/or an estimation capability limited to a common pressure range (70/110 - 80/120 mmHg).

In this paper, a novel algorithmic approach to accurately estimate both Systolic and Diastolic blood pressure (SBP, DBP) is presented. This algorithm analyzes the PPG signal acquired by non-invasive and cuff-less silicon photomultiplier sensor (SiPM), which can be installed in a commercial medical device or in a simply mobile phone.

2 THE PROPOSED BLOOD PRESSURE ESTIMATION SYSTEM

PPG signal is becoming increasingly popular in extracting cardiovascular information since it is sampled with non-invasive optical technologies

[a] https://orcid.org/0000-0003-1766-3065
[b] https://orcid.org/0000-0003-3461-4679
[c] https://orcid.org/0000-0001-6127-2470
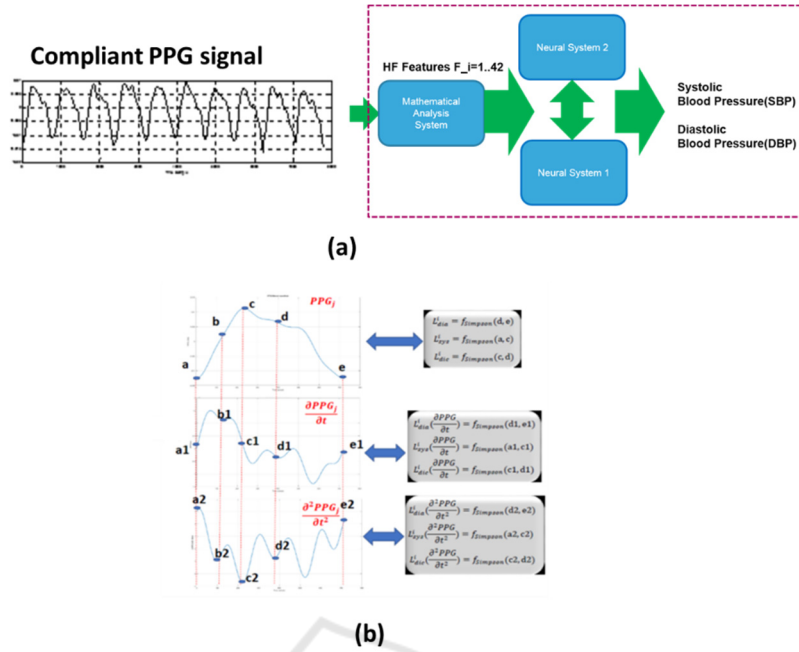[d] https://orcid.org/0000-0002-5874-7284

Figure 1: (a) BP estimation pipeline; (b) PPG and derivatives for hand crafted features.

(Vinciguerra, 2017). This signal has a great potential for the assessment of vascular diseases related to aging, hypertension, and atherosclerosis, providing information on arterial stiffness and elasticity (Oreggia, 2015).

To achieve the above reported cardiovascular information, a robust PPG signal without artifacts is mandatory. In particular, a compliant PPG waveform must comprise systolic peak (SP), dicrotic notch (DN) and diastolic peak (DP). In our previous works (Rundo, 2018) (Mazzillo, 2018) we presented a PPG pattern recognition pipeline allowing to achieve high robust PPG compliant waveform. The obtained PPG signal is herein furtherly processed to achieve a reliable BP estimation. The pipeline we used is reported in Figure 1(a). It includes a Mathematical Analysis System block, presented in (Rundo, 2018) and (Mazzillo, 2018), receiving compliant PPG signals as input. The output of this block is then learned by two layer of Neural Network (NN) providing both SBP and DBP output signals.

a) Mathematical Analysis System Block. This block is able to calculate a set of 18 features on the compliant PPG waveform and on the first and second (time) derivatives (Fig. 1 (b)). The following equations F_1 to F_{18} are exemplary of how such first act of processing can be performed in the proposed approach:

$$F_1 = \ln\left(\frac{1}{N_{PPG}}\left(\sum_{i=1}^{N_{PPG}} L_{sys}^i\right)\right) \tag{1}$$

$$F_2 = \ln\left(\frac{1}{N_{PPG}}\left(\sum_{i=1}^{N_{PPG}} L_{sys}^i\left(\frac{\partial PPG}{\partial t}\right)\right)\right) \tag{2}$$

$$F_3 = \ln\left(\frac{1}{N_{PPG}}\left(\sum_{i=1}^{N_{PPG}} L_{sys}^i\left(\frac{\partial^2 PPG}{\partial t^2}\right)\right)\right) \tag{3}$$

$$F_4 = \sigma_{L_{sys}} \tag{4}$$

$$F_5 = \sigma_{L_{sys}}\left(\frac{\partial PPG}{\partial t}\right) \tag{5}$$

$$F_6 = \sigma_{L_{sys}}\left(\frac{\partial^2 PPG}{\partial t^2}\right) \tag{6}$$

$$F_7 = \ln\left(\frac{1}{N_{PPG}}\left(\sum_{i=1}^{N_{PPG}} L_{dia}^i\right)\right) \tag{7}$$

$$F_8 = \ln\left(\frac{1}{N_{PPG}}\left(\sum_{i=1}^{N_{PPG}} L_{dia}^i\left(\frac{\partial PPG}{\partial t}\right)\right)\right) \tag{8}$$

$$F_9 = \ln\left(\frac{1}{N_{PPG}}\left(\sum_{i=1}^{N_{PPG}} L_{dia}^i\left(\frac{\partial^2 PPG}{\partial t^2}\right)\right)\right) \tag{9}$$

$$F_{10} = \sigma_{L_{dia}} \tag{10}$$

$$F_{11} = \sigma_{L_{dia}}\left(\frac{\partial PPG}{\partial t}\right) \tag{11}$$

$$F_{12} = \sigma_{L_{dia}}\left(\frac{\partial^2 PPG}{\partial t^2}\right) \tag{12}$$

$$F_{13} = \ln\left(\frac{1}{N_{PPG}}\left(\sum_{i=1}^{N_{PPG}} L_{dic}^i\right)\right) \tag{13}$$

$$F_{14} = \ln\left(\frac{1}{N_{PPG}}\left(\sum_{i=1}^{N_{PPG}} L_{dic}^i\left(\frac{\partial PPG}{\partial t}\right)\right)\right) \tag{14}$$

$$F_{15} = \ln\left(\frac{1}{N_{PPG}}\left(\sum_{i=1}^{N_{PPG}} L_{dic}^i\left(\frac{\partial^2 PPG}{\partial t^2}\right)\right)\right) \tag{15}$$

$$F_{16} = \sigma_{L_{dic}} \tag{16}$$

$$F_{17} = \sigma_{L_{dic}}\left(\frac{\partial PPG}{\partial t}\right) \tag{17}$$

$$F_{18} = \sigma_{L_{dic}}\left(\frac{\partial^2 PPG}{\partial t^2}\right) \tag{18}$$

where:

ln is (natural) logarithm; N_{PPG} are the PPF waveform samples over a period of the PPG signal; suffixes **sys**, **dia** and **dic** are the systolic, diastolic and dicrotic phases of the PPG signal identified as the portions a–b, a1–b1, a2–b2 (systolic), b–d, b1–d1,b2–d2 (dicrotic), c–e, c1-e1 and c2–e2 (diastolic) in the diagrams (PPG and its first derivative and second derivative) of Figure 1(b); $L^i x$ indicates the length of sub-curve of PPG waveform, for the systolic, diastolic and dicrotic phases **sys**, **dia** and **dic**, respectively and with i=1. N_{PPG}; in the same way, $L^i x(\partial PPG/\partial t)$ represents the length of the sub-curve of the first derivative of the PPG signal, and $L^i x$ ($\partial^2 PPG/\partial t^2$) represents the length of the sub-curve of the second derivative of the PPG signal, again for **sys**, **dia** and **dic**, respectively. For the first and second derivative of PPG signal, the Simpson rule can be adopted for computing the length of the curve (Matthews, 2004); - σ_x denotes standard deviation for variable $L^i x$.

The $F_1 - F_{18}$ features have been properly designed with the aim to have an exhaustive and analytical description of the shape of the PPG waveform. Indeed, beside common statistical indices described by features F_1, F_4, F_{10} and F_{16}, we considered specific features based on the first and second derivative of the waveform aimed to point out the peculiarities related to the directions and the inflection points of the PPG waveform, respectively.

b) Neural Systems 1 and 2. The $F_1 - F_{18}$ features are fed into the Artificial Neural Network (ANN) blocks to perform further processing to correlate the PPG signal with real SBP (systolic) and DBP (diastolic) to achieve a reliable model for BP estimation. Training

values are derived from a set of measurements performed on 30 patients in which BP was measured by conventional sphygmomanometer concurrently with the PPG signal. The first ANN (Neural System 1) is a Multi-Layer Perceptron (MLP) with a modified *Polak-Ribiere* back-propagation learning algorithm (Fletcher, 1964) (Hagan, 1996). This ANN performs a preliminary reconstruction of the blood pressure of a subject both for systolic (SBP) and diastolic (DBP) values, providing an estimation denoted as $f_1(*)$ and $f_2(*)$ for SBP and DBP respectively. The second ANN is an advanced modified version of the SOM Motor Map (Ortis, 2013), able to complete such a reconstruction of both SBP and DBP values by detecting a second estimation or component $K_1(*)$ and $K_2(*)$.

Below are reported the mathematical models used in the ANN layers:

$$SBP_{rec} = f_1\left(Polak - Ribiere\ NN\right) + K_1(w_{SBP,out}[SOM_1 - Motor\ Map]) \tag{19}$$

$$DBP_{rec} = f_2\left(Polak - Ribiere\ NN\right) + K_2(w_{DBP,out}[SOM_2 - Motor\ Map]) \tag{20}$$

Consequently, the pressure values SBPrec/DBPrec comprise a non-linear portion (f1/f2) and a linear portion (K_1/K_2).

Concerning the SOM Motor Map NN, the following equations describe the typical "Winner Take All" algorithm used for clustering the described input hand crafted PPG features:

$$w_i^{SBP,in}(x_{min}, y_{min}, t+1) = w_i^{SBP,in}(x_{min}, y_{min}, t) + \vartheta \cdot \rho(x, y, t) \cdot (F_i - w_i^{SBP,in}(x_{min}, y_{min}, t+1)) \tag{21}$$

$$w_i^{DBP,in}(x_{min}, y_{min}, t+1) = w_i^{DBP,in}(x_{min}, y_{min}, t) + \vartheta \cdot \rho(x, y, t) \cdot (F_i - w_i^{DBP,in}(x_{min}, y_{min}, t+1)) \tag{22}$$

where (x_{min},y_{min}) represents the coordinates of the neurons which minimize the Euclidian distance between the input weights and the related hand crafted input vector while " ϑ " and " $\rho(x, y, t)$ " represents the learning rate and neighborhood function (gaussian) of the WTA algorithm. This winner neuron produces the related output per following equation:

Table 1: DBP and SBP Results.

Patient Number	Age	Pathologies	Actual Blood Pressure (DBP/SBP)	Estimated Blood Pressure (DBP$_{rec}$/SBP$_{rec}$)
1	32	No	85/123	83.21/121.11
2	24	No	80/120	79.22/122.53
3	53	Yes	85/125	83.98/123.24
4	65	Yes	90/135	91.09/132.99
5	46	No	70/120	68.92/119.87
6	33	No	80/115	78.81/115.09
7	21	No	70/105	69.04/104.98
8	52	Yes	90/130	89.01/132.21
9	25	No	80/130	78.99/131.09
10	58	No	85/130	83.93/129.91

$$w_{SBP,out}(x_{min}, y_{min}, t+1)$$
$$= w_{SBP,out}(x_{min}, y_{min}, t) + \vartheta$$
$$\cdot \sum \rho(x, y, t) \quad (23)$$
$$\cdot ([SBP - f_1(Polak - Ribiere\ NN)]$$
$$- w_{SBP,out}(x_{min}, y_{min}, t)$$

$$w_{DBP,out}(x_{min}, y_{min}, t+1)$$
$$= w_{DBP,out}(x_{min}, y_{min}, t) + \vartheta$$
$$\cdot \sum \rho(x, y, t) \quad (24)$$
$$\cdot ([DBP - f_2(Polak - Ribiere\ NN)$$
$$- w_{DBP,out}(x_{min}, y_{min}, t))$$

We compute the following learning errors:

$$E^{DBP}(t+1) = \frac{1}{2}(DBP(t+1) - DBP_{rec}(t+1))^2 \quad (25)$$

$$E^{SBP}(t+1) = \frac{1}{2}(SBP(t+1) - SBP_{rec}(t+1))^2 \quad (26)$$

If the above error functions are progressive decreasing (i.e., the conditions in Equation (27) and Equation (28) are satisfied), the related weights update will be confirmed and then we have Equation (29) and Equation (39). Otherwise, both input and output weight updates will be discarded.

$$E^{DBP}(t+1) < E^{DBP}(t) \quad (27)$$

$$E^{SBP}(t+1) < E^{SBP}(t) \quad (28)$$

$$w_{SBP,out}(x_{min}, y_{min}, t+1) = K_1(w_{SBP,out}) \quad (29)$$

$$w_{DBP,out}(x_{min}, y_{min}, t+1) = K_2(w_{SBP,out}) \quad (30)$$

3 RESULTS

This study was conducted in accordance with the Helsinki Declaration of 1975. All patients provided written informed consent before enrollment. The study was approved by the Ethical Committee Catania 1 (Authorization No. 113/2018/PO).

Table 2: Average errors of the proposed algorithm.

Blood Pressure	Average Error
DBP	2.718 mmHg
SBP	2.853 mmHg

We engaged 30 patients having different genders (male and female), ages (between 20 and 70 years old) and pathologies (we collected healthy subjects and sick ones with different issues such as cardiac problems, hypertension, diabetes, etc.).

Table 1 and Table 2 show SBP and DBP values and the average error the obtained by the proposed approach, respectively. The average error for both estimation (SBP and DBP) is less than 3 mmHg corresponding to about 10/15 % of real measure. This is an acceptable result from a medical point of view and with respects to prior state of the art above mentioned.

4 CONCLUSIONS

In this paper we proposed a novel algorithmic for non-invasive cuff-less BP estimation, easily embedded in several kind of devices from mobile to portable medical systems. This algorithm takes the PhotoPlethysmoGraphy (PPG) signal as input, acquired by miniaturized silicon photomultiplier SiPM devices. The PPG data are processed with *ad-hoc* bio-inspired mathematical model which estimates both systolic and diastolic pressure values. We compared our results with the measures obtained by using a classical sphygmomanometer device, achieving a mean accuracy of 97%. Hence, the performances achieved by the proposed method are suitable for clinical use.

Future works aim to improve better the estimation increasing the training set number and the type of neural system we used. Further efforts will be also devoted to the extension of the experiments, by a comparative evaluation among a set of state-of-the-art methods on a proper large-scale benchmark dataset.

REFERENCES

Kurylyak, Y., Lamonaca, F., and Grimaldi, D. (2013, May). A neural network-based method for continuous blood pressure estimation from a PPG signal. In *2013 IEEE International instrumentation and measurement technology conference (I2MTC)* (pp. 280-283). *IEEE*.

Y Yan, Y. S., and Y. T. Zhang. "Noninvasive estimation of blood pressure using photoplethysmographic signals in the period domain." *2005 IEEE Engineering in Medicine and Biology 27th Annual Conference. IEEE*, 2006.

Gu, W. B., C. C. Y. Poon, and Y. T. Zhang. "A novel parameter from PPG dicrotic notch for estimation of systolic blood pressure using pulse transit time." *2008 5th International Summer School and Symposium on Medical Devices and Biosensors. IEEE, 2008*.

Teng, X. F., and Y. T. Zhang. "Continuous and noninvasive estimation of arterial blood pressure using a photoplethysmographic approach." *Proceedings of the 25th Annual International Conference of the IEEE Engineering in Medicine and Biology Society (IEEE Cat. No. 03CH37439). Vol. 4. IEEE, 2003*.

Fortino, G., and Giampà, V. (2010, April). PPG-based methods for non-invasive and continuous blood pressure measurement: an overview and development issues in body sensor networks. In *2010 IEEE International Workshop on Medical Measurements and Applications (pp. 10-13). IEEE.*

Vinciguerra, V., Ambra, E., Maddiona, L., Oliveri, S., Romeo, M. F., Mazzillo, M., Rundo, F., and Fallica, G. (2017, September). Progresses towards a processing pipeline in photoplethysmogram (PPG) based on SiPMs. In *2017 European Conference on Circuit Theory and Design (ECCTD) (pp. 1-5). IEEE.*

Oreggia, D., Guarino, S., Parisi, A., Pernice, R., Adamo, G., Mistretta, L., Di Buono, P., Fallica, G., Cino, C. and Busacca, A.. Physiological parameters measurements in a cardiac cycle via a combo PPG-ECG system. *Proceedings of the AEIT International Annual Conference, 2015*; pp. 1-6;

Rundo, F., Conoci, S., Ortis, A., Battiato, S. "An Advanced Bio-Inspired PhotoPlethysmoGraphy (PPG) and ECG Pattern Recognition System for Medical Assessment". *Sensors 2018*, 18, 405.

Mazzillo, M., Maddiona, L., Rundo, F., Sciuto, A., Libertino, S., Lombardo, S., and Fallica, G. (2018). Characterization of SiPMs with NIR long-pass interferential and plastic filters. *IEEE Photonics Journal*, 10(3), 1-12.

Matthews, John H. (2004). "Simpson's 3/8 Rule for Numerical Integration". Numerical Analysis - Numerical Methods Project. *California State University, Fullerton. Archived from the original on 4 December 2008.* Retrieved 11 November 2008.

Fletcher, Reeves, and Colin M. Reeves. "Function minimization by conjugate gradients." *The computer journal 7.2* (1964): 149-154.

Hagan, M. T., Demuth, H. B., Beale, M. H., & De Jesús, O. (1996). Neural network design (Vol. 20). *Boston: Pws Pub.*

Ortis A., Rundo F., Di Giore G., Battiato S. (2013) Adaptive Compression of Stereoscopic Images. In: Petrosino A. (eds) Image Analysis and Processing – ICIAP 2013. *ICIAP 2013. Lecture Notes in Computer Science, vol 8156. Springer, Berlin, Heidelberg.*